

## LIST OF ILLUSTRATIONS

Figure 1.1. Distribution of the Karoo Supergroup within the Karoo Basin and elsewhere in Southern Africa. The section line X-X' is shown in Figure 1.5 (modified after Tankard <i>et al.</i> , 1982). . . . .	3
Figure 1.2. Locality map of the study area. . . . .	4
Figure 1.3. Locality map of the study area within the Highveld Coalfield (modified after Jordaan, 1986). . . . .	5
Figure 1.4. Borehole location map, illustrating the density of boreholes available for this study, and the data limits. . . . .	8
Figure 1.5. North-east South-west cross-section (Figure 1.1) through the Karoo Basin showing: (A) Distribution of the major lithological units, (B) Major depositional systems (modified after Tankard <i>et al.</i> , 1982).	11
Figure 1.6. The development and ages of coal seams in various Karoo Basins in South Africa (modified after Falcon, 1986). . . . .	12
Figure 1.7. Map showing the inferred ice centres of the Late-Carboniferous ice. The arrows indicate observed glacial striae. A, Namaqualand; B, Griqualand West; C, Northern Province; and D, Kwa Zulu-Natal ice centres (modified after du Toit, 1954). . . . .	14
Figure 2.1. The stratigraphic column and depositional sequences of the Highveld Coalfield (modified after Winter, 1985). . . . .	22

Figure 2.2. Typical stratigraphic columns, illustrating the stratigraphic variations for different parts of the Highveld Coalfield, compared to the study area. . . . .	24
Figure 2.3. Typical stratigraphic column for the New Denmark study area. . . . .	25
Figure 2.4 Typical graphic log for the No. 4 seam at New Denmark Colliery. . . . .	26
Figure 3.1. Diamictite sub-facies comprising a siltstone matrix and extrabasinal pebbles. . . . .	33
Figure 3.2. Clast supported sub-facies of the conglomerate facies containing small-pebbles of quartz and feldspar. . . . .	35
Figure 3.3. Roundness and sphericity scale (modified after Folk, 1974)..	36
Figure 3.4. Matrix-supported sub-facies of the conglomerate facies comprising quartz and feldspar grains. The unit is coarsening-upward.	37
Figure 3.5. Cross-bedded small-pebble conglomerate sub-facies comprising poorly-sorted quartz and feldspar grains. . . . .	39
Figure 3.6 (A) Well-sorted coarse- to medium-grained sandstone. The absence of structure appears to be primary. (B) Coarse sandstone with shale rip-up clasts. . . . .	41
Figure 3.7. Massive sandstone sub-facies, (A) Illustrates well-sorted, fine-grained sandstone, (B) Well-sorted, medium-grained sandstone. . . . .	42

Figure 3.8. (A) Planar cross-bedded sandstone sub-facies. The cross-bedding is defined by fining-upward foresets, (B) Planar cross-bedding with cm-intrabedded conglomerate lag and coal-spar lenses at the top. . . . .	44
Figure 3.9. Trough cross-bedded sandstone sub-facies defined by scoured surfaces, with concave laminae. . . . .	46
Figure 3.10. (A) Planar laminated sandstone sub-facies illustrating well defined horizontal to sub-horizontal laminae. . . . .	48
Figure 3.11. (A) Cross-laminated sandstone sub-facies, wave-ripple lamination, capped by siltstone, (B) Cross-laminated sandstone-siltstone with some soft-sediment deformation structures present. . . . .	50
Figure 3.12. Cross-lamination produced by current ripples. . . . .	52
Figure 3.13. (A) Cross-bedded glauconite sandstone sub-facies with a few siltstone lenses, and (B) with a siltstone layer at the bottom. Note the green glauconite grains that are clearly visible on the cross-section of the core. . . . .	54
Figure 3.14. Bioturbated sandstone sub-facies, with interlaminated dark-grey siltstone. Both lithologies have been intensively bioturbated. . . . .	56
Figure 3.15. Block diagram showing (a) Flaser, (b) Wavy, and (c) Lenticular lamination (modified after Davis, 1983). . . . .	59
Figure 3.16. Flaser laminated sandstone facies within the cross-laminated sandstone sub-facies. . . . .	61

Figure 3.17. Wavy-laminated sandstone-siltstone sub-facies and erosional contact, (B) Sandstone-siltstone facies illustrating well defined horizontal laminae. . . . .	63
Figure 3.18. (A) Lenticular-laminated siltstone with sandstone lenses, (B) The same sub-facies with a 2cm diagenetic pyrite nodule. . . . .	65
Figure 3.19. Siltstone facies. This core sample contains interlaminated sandstone-siltstone at the top. . . . .	67
Figure 3.20. Gravelly siltstone sub-facies. . . . .	68
Figure 3.21. Carbonaceous siltstone sub-facies. . . . .	72
Figure 3.22. No. 4 seam coal facies at New Denmark showing dull and bright bands.. . . .	74
Figure 4.1. Locality map showing the positions of cross-sections. . . . .	79
Figure 4.2. West-east cross-section A-B of the No. 4 seam depositional sequence. See Figure 4.1 for the location of cross-section. . . . .	80
Figure 4.3. West-east cross-section C-D of the No. 4 seam depositional sequence. See Figure 4.1 for the location of cross-section. . . . .	81
Figure 4.4. West-east cross-section E-F of the No. 4 seam depositional sequence. See Figure 4.1 for the location of cross-section. . . . .	82
Figure 4.5. Northeast/southwest cross-section G-H of the No. 4 seam depositional sequence. See Figure 4.1 for the location of cross-section. . . . .	83

Figure 4.6	Carbonaceous siltstone with minor coal seams followed by small-pebble conglomerate material at the top.	85
Figure 4.7.	The erosive base of a channel sequence between No. 4 and No. 4 A coal seams. Very coarse-grained, poorly sorted sandstone can be seen scouring into the underlying carbonaceous siltstone. Figures 4.2-4.5 illustrate the lateral extent of these erosive units.	87
Figure 4.8.	Classification of depositional continental environments and their associated depositional models (modified after Conybeare, 1979).	88
Figure 4.9.	Block diagrams illustrating a meandering river and its floodplain (modified after Blatt <i>et al.</i> , 1980).	90
Figure 4.10.	A conceptual framework relating deltaic facies patterns to delta morphology, regime and nature of the basin (modified after Colella and Prior, 1990).	93
Figure 4.11.	Classification of depositional transitional environments and their associated depositional models (modified after Conybeare, 1979).	94
Figure 4.12.	Twelve major prototype deltas being dominated by fluvial processes (modified after Colella and Prior, 1980).	97
Figure 5.1.	Borehole core at the drilling site in the north-eastern part of the study area at New Denmark. The borehole core includes a complete sequence. See Figures 4.2-4.5 for the lithostratigraphic classification of this sequence. Note core is in 10m intervals.	105

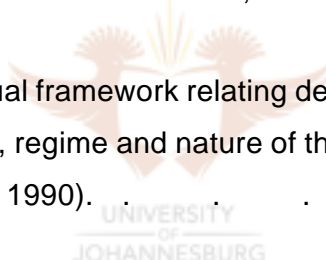


Figure 5.2. Grit lenses within carbonaceous siltstone. Note erosive contacts. . . . .	106
Figure 5.3. West-east cross-section above the No. 4 coal seam illustrating the coarse-grained fluvial channel deposits above No. 4 seam . . . . .	109
Figure 5.4. Contact between the roof of No. 4 coal seam and overlying pebbly sandstone. Note bar-scale in 10cm intervals. . . . .	110
Figure 5.5. Fluvial depositional sequences above No. 4 coal seam. Note bar-scale in 10cm intervals. . . . .	111
Figure 5.6. Erosional contact of fluvial sandstone and conglomerates forming the immediate roof of No. 4 coal seam. Note the coal-spar rip-up clast approximately 25cm and 8m from the base of the succession. Note bar-scale in 10cm intervals. . . . .	113
Figure 5.7. Locality map showing the positions of cross-sections (Figures 5.8-5.12) used to illustrate the details of the facies assemblages in the roof above No. 4 seam. . . . .	115
Figure 5.8. West-east cross-section A-B above the No. 4 coal seam depositional sequence. See figure 5.7 for the location of cross-section. . . . .	116
Figure 5.9. West-east cross-section C-D above the No. 4 coal seam depositional sequence. See figure 5.7 for the location of cross-section. . . . .	117
Figure 5.10. West-east cross-section E-F above the No. 4 coal seam depositional sequence. See figure 5.7 for the location of cross-section. . . . .	118

Figure 5.11. North-south cross-section G-H above the No. 4 coal seam depositional sequence. See figure 5.7 for the location of cross-section. . . . .	119
Figure 5.12. Southwest-northeast cross-section I-J above the No. 4 coal seam depositional sequence. See figure 5.7 for the location of cross-section. . . . .	120
Figure 5.13. Isopach map of the No. 4 coal seam in the New Denmark study area. . . . .	123
Figure 5.14. Isopach of the conglomerate facies directly above the No. 4 coal seam depositional sequence. The facies thins towards the west and thickens eastwards. . . . .	125
Figure 5.15. Isopach of sandstone-siltstone directly below the glauconite stratigraphic marker. . . . .	126
Figure 5.16. The mine hazard plan overlying conglomerate facies directly above No. 4 seam. . . . .	127
Figure 5.17. (A) Rider coal above No. 4 coal seam, within the massive to pebbly sandstone. (B) Note also detailed view of the rider coal. Noting these features in core can aid in planning of appropriate roof support. . . . .	132